

# ~~Measurement Report~~: Tropospheric and Stratospheric Ozone Profiles during the 2019 TROPomi vaLIdation eXperiment (TROLIX-19)

John T. Sullivan<sup>1</sup>, Arnoud Apituley<sup>2</sup>, Nora Mettig<sup>3</sup>, Karin Kreher<sup>4</sup>, K. Emma Knowland<sup>1,5</sup>, Marc Allaart<sup>2</sup>, Ankie Piters<sup>2</sup>, Michel Van Roozendaal<sup>6</sup>, Pepijn Veeffkind<sup>2</sup>, Jerry R. Ziemke<sup>1,5</sup>, Natalya Kramarova<sup>1</sup>, Mark Weber<sup>3</sup>, Alexei Rozanov<sup>3</sup>, Laurence Twigg<sup>1,7</sup>, Grant Sumnicht<sup>1,7</sup>, and Thomas J. McGee<sup>1\*</sup>

<sup>1</sup> NASA Goddard Space Flight Center, Greenbelt, MD 20771

<sup>2</sup> Royal Netherlands Meteorological Institute (KNMI), De Bilt, Netherlands

<sup>3</sup> Institute of Environmental Physics, University of Bremen, Bremen, Germany

<sup>4</sup> BK Scientific GmbH, Mainz, Germany

<sup>5</sup> Morgan State University/GESTAR-II, Baltimore, MD 21251

<sup>6</sup> Belgian Institute for Space Aeronomie (BIRA), Ukkel, Belgium

<sup>7</sup> Science Systems and Applications Inc., Lanham, MD, 20706

\*Now Emeritus

*Correspondence to:* John Sullivan (john.t.sullivan@nasa.gov)

**Abstract** A TROPospheric Monitoring Instrument (TROPOMI) validation campaign was held in the Netherlands based at the CESAR (Cabauw Experimental Site for Atmospheric Research) Observatory during September 2019. The TROPomi vaLIdation eXperiment (TROLIX-19) consisted of active and passive remote sensing platforms in conjunction with several balloon-borne and surface chemical (e.g. ozone and nitrogen dioxide) measurements. The goal of this joint NASA-KNMI geophysical validation campaign was to make intensive observations in the TROPOMI domain in order to be able to establish the quality of the L2 satellite data products under realistic conditions, such as non-idealized conditions with varying cloud cover and a range of atmospheric conditions at a rural site. The research presented here focuses on using ozone lidars from NASA's Goddard Space Flight Center to better evaluate the characterization of ozone throughout TROLIX-19. Results of comparisons to the lidar systems with balloon, space-borne, and ground-based passive measurements are shown. In addition, results are compared to a global coupled chemistry meteorology model to illustrate the vertical variability and columnar amounts of both tropospheric and stratospheric ozone during the campaign period.

## 31 **1 Introduction**

32 In September 2019, a joint Royal Netherlands Meteorological Institute (KNMI) and the U.S. National  
33 Aeronautics and Space Administration (NASA) field campaign was performed in the Netherlands, based  
34 at the Cabauw Experimental Site for Atmospheric Research (CESAR, 51.97° N, 4.93° E), to provide the  
35 scientific community with additional information to further understand and evaluate the Copernicus  
36 Sentinel-5 Precursor mission (S-5P) TROPOspheric Monitoring Instrument (TROPOMI) instrument  
37 (<https://sentinels.copernicus.eu/web/sentinel/missions/sentinel-5p>). The main objective of the  
38 Copernicus Sentinel-5P mission is to perform atmospheric measurements with high spatio-temporal  
39 resolution, to be used for scientific studies and monitoring of air quality and chemical transport  
40 ([https://www.esa.int/Applications/Observing\\_the\\_Earth/Copernicus/Sentinel-5P](https://www.esa.int/Applications/Observing_the_Earth/Copernicus/Sentinel-5P)).

41 To properly support satellite evaluation, the 2019 TROPomi vaLIdation eXperiment (TROLIX-19)  
42 campaign was designed to bring together many active and passive remote sensing platforms in  
43 conjunction with several balloon-borne, airborne and surface measurements. Specifically, the  
44 observations were established to provide geophysical verification in order to establish the quality of  
45 TROPOMI Level 2 (L2) main data products under realistic non-idealized conditions with varying cloud  
46 cover and a wide range of atmospheric conditions. Cabauw, using its comprehensive in-situ and remote  
47 sensing observation program in and around the 213 m meteorological tower ([https://ruisdael-  
48 observatory.nl/trolix19-tropomi-validation-experiment-2019/](https://ruisdael-observatory.nl/trolix19-tropomi-validation-experiment-2019/)) was the main site of the campaign with  
49 focus on vertical profiling using lidar instruments for aerosols, clouds, water vapor, tropospheric and  
50 stratospheric ozone, as well as balloon-borne sensors for nitrogen dioxide (NO<sub>2</sub>) and ozone (Figure 1).  
51 Although this work focuses primarily on the ozone lidar profiling during the study, the larger campaign  
52 overview, background, and motivation can be found in Apituley *et al.* (2019; 2020) or Kreher *et al.*  
53 (2020a).

54 One main goal of this work is also to understand ozone profile retrievals as they relate to upcoming  
55 satellite endeavors. As NASA prepares to launch its first geostationary air quality satellite “Tropospheric

56 Emissions: Monitoring of Pollution” (TEMPO<sub>2</sub>) this work also specifically establishes a paradigm of  
57 evaluation for TEMPO-derived products such as tropospheric ozone columns and a 0-2km tropospheric  
58 ozone product. An analogous geo-stationary air quality satellite, the Copernicus Sentinel-4 mission (S-  
59 4), <https://sentinels.copernicus.eu/web/sentinel/missions/sentinel-4>, will provide hourly data on  
60 tropospheric constituents over Europe and the CESAR site is directly within the satellite’s field of  
61 regard. Due to the finer spatial footprint, increased temporal frequency and vertical extent of  
62 TEMPO’s the TEMPO tropospheric ozone retrievals, ozone lidars are an ideal platform to perform future  
63 evaluations of the products, which builds from recent work done in Johnson *et al.*, 2018. Specifically,  
64 this work will investigate the results from the combination of having a co-located NASA tropospheric  
65 (Sullivan *et al.*, 2014) and stratospheric ozone lidars (McGee *et al.*, 1991) in order to obtain an entire  
66 vertical profile of ozone from ~0.2km to 50km.

67 For the first time, this transportable combination of lidars is able to explicitly derive diurnally varying  
68 tropospheric and total ozone columns, which are compared directly to measurements obtained by  
69 ground-based passive sensors, current satellite instrumentation and chemical transport models. In  
70 Section 2 we present all available data and methods used in this work, across the various platforms  
71 during the TROLIX-19 study. Section 3 focuses on comparisons of the tropospheric ozone retrievals of  
72 the vertical profiles of ozone within the troposphere and columnar reductions of 0-10 km and 0-2 km.  
73 Comparisons of lidar data with available complete ozone profiles (Sec 4) and columnar amounts (Sec 5)  
74 from several platforms and chemical transport models are also presented to further understand the  
75 quality of satellite derived ozone profiles during the TROLIX-19 period.

76

## 77 2 Data and Methods

78 Descriptions of the various observational and model data sets and used in this study are below, including  
79 a summary table (Table 1).

## 80 2.1 NASA Ozone Differential Absorption Lidars (DIAL)

81 NASA deployed and operated two ozone lidars during TROLIX-19 at the Cabauw site near the CESAR  
82 tower to observe temporal and vertical gradients in tropospheric and stratospheric ozone. This was the  
83 first dual-deployment of these lidars, in which the tropospheric ozone lidar measured between the near  
84 surface (about 0.2 km) to a height of about 18 km and the stratospheric lidar during night-time from 15  
85 km upwards to nearly 50 km, providing complete hybrid ozone profiles for the campaign period.

86 Measurements were made during periods of mostly clear skies, although occasional cloud cover did  
87 enter the measurement period.

88 The NASA GSFC Mobile Stratospheric Ozone Lidar Trailer Experiment (STROZ-LITE) has been a  
89 participant in the Network for the Detection of Atmospheric Composition Change (NDACC) since its  
90 inception and is housed in a 12.5m container allowing for transport around the world (McGee et al.,  
91 1991). The lidar instrument transmits two wavelengths, 308 nm from a XeCl excimer laser, and 355 nm  
92 from a ND:YAG laser to derive ozone number density profiles, which have historically served as an  
93 intercomparison data set for other NDACC ozone lidars (recent intercomparison can be found at Wing *et*  
94 *al.*, 2020; 2021).

95 The NASA GSFC TROPOZ has been developed in a transportable 13.5m trailer to take routine  
96 measurements of tropospheric ozone near the Baltimore–Washington, D.C. area as well as various  
97 campaign locations (Sullivan *et al.*, 2014; 2015,2019, Leblanc *et al.*, 2018). This instrument, which  
98 utilizes a ND:YAG laser and Raman cell, has been developed as part of the ground-based Tropospheric  
99 Ozone Lidar NETwork (TOLNet, <https://www-air.larc.nasa.gov/missions/TOLNet/>), which currently  
100 consists stations across the North America (<http://www-air.larc.nasa.gov/missions/TOLNet/>). The  
101 primary purposes of the instruments within TOLNet are to provide regular, high-fidelity profile  
102 measurements of ozone within the troposphere for satellite and model evaluation. This lidar also  
103 operates routinely for the Network for the Detection of Atmospheric Composition Change (NDACC).

104 [More than thirty NDACC ground-based Lidar instruments](#)  
105 [\(https://lidar.jpl.nasa.gov/ndacc/index\\_ndacc.php\)](https://lidar.jpl.nasa.gov/ndacc/index_ndacc.php) deployed worldwide from Pole to Pole are  
106 [monitoring atmospheric ozone, temperature, aerosols, water vapor, and polar stratospheric clouds.](#)

107 Both lidars collect backscattered radiation with a large primary telescope and a 10cm telescope for near  
108 field channels. Spectral separation is accomplished using dichroic beam-splitters and interference filters.  
109 For the stratospheric system, five return wavelengths are recorded: the two transmitted wavelengths, and  
110 the nitrogen Raman scattered radiation from each of the transmitted beams 332 nm and 382 nm, and the  
111 408 nm water vapor channel. In this arrangement for TROLIX-19, the tropospheric system pumped the  
112 Raman cell with the fourth harmonic (266 nm), which resulted in conversion to 289 nm and 299 nm  
113 using a single hydrogen/deuterium Raman cell. All of the signals are further split to improve the  
114 dynamic range of the respective lidar optical detection chains and are then amplified, discriminated and  
115 recorded using photon counting techniques.

116 During TROLIX-19, the STROZ-LITE was operated on cloud free nights, with measurements lasting  
117 between 2-4 hours to obtain enough signal to properly retrieve the entire stratospheric ozone profile. The  
118 TROPOZ was operated during daytime and night time to provide tropospheric ozone profiles. For  
119 instances of TROPOMI overpasses, campaign ozonesondes, or coincident stratospheric ozone lidar  
120 measurements, the TROPOZ reported data is averaged for 30 minutes, centered around the satellite  
121 overpass or launch time. This temporal period of averaging has been optimized in several cases to avoid  
122 cloud contamination. For all other times during the TROPOZ operation, the data has been averaged to  
123 10 minutes, which is suitable under most clear sky conditions to retrieve ozone information within the  
124 entire troposphere. [A brief description and community standardized definitions of the uncertainty budget](#)  
125 [of the lidar measurements presented in this paper can be found in Sullivan \*et al.\*, 2014, Leblanc \*et al.\*,](#)  
126 [2016 and Leblanc \*et al.\*, 2018. The maximum statistical uncertainties for the two GSFC lidars vary from](#)  
127 [night to night depending on atmospheric conditions and laser power fluctuations. They are mostly within](#)  
128 [10-20% for 5 min and 5-8% for 30 min integrations throughout the atmosphere. Within overlapping](#)

129 measurement regions in the upper troposphere/lower stratosphere, they are different at the same altitude  
130 due to laser performance and telescope/detector efficiency differences, and are therefore joined  
131 manually for this work based on appropriate signal to noise and uncertainty estimates.

## 132 **2.2 Ground Based Passive Sensors and Ozonesondes**

### 133 **2.2.1 Pandora Spectrometer Instrument**

134 A Pandora spectrometer instrument (#118) has been used to measure columnar amounts of trace gases in  
135 the atmosphere at 3–5-minute resolution at the Cabauw site since 2016 and previously used for the  
136 second Cabauw Intercomparison of Nitrogen Dioxide (CINDI-2) campaign (Kreher et al., ~~2020b~~2020).  
137 Using the theoretical solar spectrum as a reference, Pandora determines trace gas amounts using  
138 differential optical absorption spectroscopy (DOAS). This attributes in principal these differences in  
139 spectra measured by Pandora to the presence of trace gases within the atmosphere (*i.e.* the difference  
140 between the theoretical solar spectrum and measured spectrum is caused by absorption of trace gas  
141 species). For this study, L2 direct sun columnar values of ozone are used, although retrievals of nitrogen  
142 dioxide are also operationally acquired. Data used passed the strictest QC/QA estimate (Flags = 10) and  
143 was obtained from the Pandonia Global Network (<http://data.pandonia-global-network.org/>).

### 144 **2.2.2 Brewer MKIII Spectrophotometer**

145 A Brewer MKIII spectrometer instrument (#189) has been used to measure daily columnar amounts of  
146 ozone in the atmosphere at the KNMI/De Bilt (30km NE of Cabauw) ~~site since 2007.~~, 52.10° N, 5.18°  
147 E). Brewer #189 has been operated continuously since 1 October 2006. It replaced Brewer #100 which  
148 provided observations since 1 January 1994. De Bilt has the longest continuous record of ozone  
149 measured with an MKIII instrument in the World Ozone and Ultraviolet Radiation Data Centre  
150 (WOUDC) database.

151 The Brewer is specifically designed to provide high accuracy measurement of spectrally resolved UV  
152 for satellite evaluation, climatology monitoring and public health to international standards. Similar to  
153 Pandora spectrometers, these measurements of total column of trace gases are compared to the measured  
154 UV spectrum with the known solar output, and modeling the scattering properties of the atmosphere and  
155 have been historically used to evaluate columnar satellite products (McPeters *et al.*, 2007; Wenig *et al.*,  
156 2008; Garane *et al.*, 2019). The Brewer is the standard instrument used in the [World Meteorological  
157 Organization](#) ozone monitoring network and for NDACC. This data was obtained at the NDACC  
158 website (<https://www-air.larc.nasa.gov/missions/ndacc/data.html>).

### 159 **2.2.3 Ozonesondes**

160 Ozonesondes have been used to measure vertical profiles of ozone in the atmosphere at the KNMI/De  
161 Bilt (30km NE of Cabauw) site since November 1992, and measurements are made weekly, historically  
162 at 12 UTC on Thursdays. Description of the Electro Chemical Cell (ECC) details and metadata are  
163 summarized in Malderen *et al.*, 2016, which also describes the importance of understanding and  
164 reporting changes in ozonesonde operation procedures. During the [campaign](#), in situ  
165 measurements of ozone were made using a balloon-borne payload consisting of an ECC ozonesonde  
166 (Science Pump Corporation, [Serial Numbers: 6A35438, 6A35447, 6A35448, 6A35441](#)) coupled with a  
167 radiosonde ([Vaisala RS41](#)) and have been used to evaluate TROPOMI tropospheric ozone products in  
168 the tropics (Hubert *et al.*, 2021). The ECC technique is widely used for the high vertical resolution  
169 measurements of O<sub>3</sub>. The ECC consists of two chambers with platinum electrodes immersed in  
170 potassium iodide (KI) solutions at different concentrations. The accuracy in the O<sub>3</sub> concentration  
171 measured by an ECC ozonesonde is  $\pm 5\%$ – $10\%$  up to an altitude of 30 km (Smit *et al.*, 2007); [Smit and  
172 Thompson \*et al.\*, 2021](#)). This data was obtained at the NDACC website ([https://www-  
air.larc.nasa.gov/missions/ndacc/data.html](https://www-<br/>173 air.larc.nasa.gov/missions/ndacc/data.html)).

## 174 2.3 Satellite Observations and Products

175 Satellite data used in this work was selected based on the closest retrieval (*i.e.* column, profile) to the  
176 CESAR station within +/-2.5 degrees latitude and +/-10 degrees in longitude.

### 177 2.3.1 Ozone Mapping and Profiling Suite (OMPS) and MERRA-2 products

178 ~~Daily total column ozone overpasses over Cabauw station from the~~ The Ozone Mapping and  
179 ~~Profiling Profiler~~ Suite (OMPS) ~~Nadir Mapper (NM) instrument~~ on the Suomi National Polar-orbiting  
180 Partnership (S-NPP) platform ~~are used~~ consists of three sensors to measure the total column and the  
181 vertical distribution of ozone with high spatial and vertical resolutions (Flynn et al., 2006). Daily total  
182 column ozone overpasses over Cabauw station from the OMPS Nadir-Mapper (NM) instrument are used  
183 in this study. The vertical distribution of ozone in the stratosphere and lower mesosphere is obtained  
184 from the OMPS Limb-Profiler (LP) sensor on the Suomi-NPP satellite merging the UV (29.5-52.5 km)  
185 and VIS (12.5-35.5 km) bands to provide a full profile from 12.5km to 52.5km (Kramarova *et al.*, 2018).  
186 Variations of this merged OMPS-LP retrieval were considered, however the work shown in Arosio *et*  
187 *al.*, 2018, indicates the same overall conclusions would be reached. Further work beyond this manuscript  
188 may involve comparing this TROLIX-19 measurement data set to specific experimentally performed  
189 satellite retrievals.

190 The Modern-Era Retrospective analysis for Research and Applications, Version 2 (MERRA-2) provides  
191 data beginning in 1980 and since August 2004 assimilates NASA's satellite ozone profile observations  
192 from Aura Microwave Limb Sounder (MLS) (Livesey et al, 2008) to more comprehensively characterize  
193 stratospheric ozone abundance. A residual tropospheric ozone product (Ziemke *et al.*, 2019) is derived  
194 using the OMPS NM total column ozone minus the co-located MERRA-2 stratospheric column ozone.  
195 Tropopause pressure is derived from MERRA-2 potential vorticity (2.5 PVU) and potential temperature  
196 (380 K).



### 197 **2.3.3 MLS**

198 NASA's Aura Microwave Limb Sounder (MLS) uses microwave emission to measure stratospheric  
199 and upper tropospheric constituents, such as ozone. Ozone data (v5) used in this study is binned on  
200 various vertical grids and are converted from volume mixing ratio to number density using the  
201 coincident MERRA-2 atmosphere state parameters. Both daytime and nighttime data are used in this  
202 study and the corresponding closest profile is utilized for comparison.

### 203 **2.3.4 TROPOMI**

204 In October 2017, the Sentinel-5 Precursor (S5P) mission was launched, carrying the TROPospheric  
205 Monitoring Instrument (TROPOMI), which is a nadir-viewing 108° Field-of-View push-broom grating  
206 hyperspectral spectrometer. Starting in August 2019, Sentinel-5P TROPOMI along-track high spatial  
207 resolution (approximately 5.5 km at nadir) has been implemented and total ozone columns values used  
208 in this work are subsetted from the NASA GES DISC  
209 ([https://tropomi.gesdisc.eosdis.nasa.gov/data/S5P\\_TROPOMI\\_Level2/S5P\\_L2\\_\\_O3\\_TOT\\_HiR.1/](https://tropomi.gesdisc.eosdis.nasa.gov/data/S5P_TROPOMI_Level2/S5P_L2__O3_TOT_HiR.1/)) to  
210 provide the Offline 1-Orbit L2 (S5P\_L2\_\_O3\_TOT\_HiR), which is based on the Direct-fitting algorithm  
211 (S5P\_TO3\_GODFIT), comprising a non-linear least squares inversion by comparing the simulated and  
212 measured backscattered radiances.

213 Tropospheric Ozone vertical profiles were retrieved using the TOPAS (Tikhonov regularized Ozone  
214 Profile retrieval with SCIATRAN) algorithm and were applied to the TROPOMI L1B spectral data  
215 version 2, using spectral data between 270 and 329 nm for the retrieval (Mettig *et al.*, 2021). This data  
216 set will cover the TROLIX-19 period from 09 September until 28 September; however, it is available  
217 outside of this work for specific weeks between June 2018 and October 2019. Since the ozone profiles  
218 are very sensitive to absolute calibration at short wavelengths, a re-calibration of the measured radiances  
219 is required using comparisons with simulated radiances with ozone limb profiles from collocated  
220 satellites used as input. The a priori profiles for ozone are taken from the ozone climatology of Lamsal

221 et al. (2004) and the calibration correction spectrum is determined using the radiances modelled with  
222 ozone information from collocated MLS/Aura measurements as described in depth throughout Mettig *et*  
223 *al.*, 2021.

224

## 225 **2.4 Coupled Chemistry and Meteorology Model**

226 The GEOS Composition Forecasting (GEOS-CF, [https://gmao.gsfc.nasa.gov/weather\\_prediction/GEOS-](https://gmao.gsfc.nasa.gov/weather_prediction/GEOS-)  
227 [CF/](https://gmao.gsfc.nasa.gov/weather_prediction/GEOS-CF/), Keller *et al.*, 2021, Knowland *et al.*, 2021) system was chosen to serve as a comparison simulation  
228 for this effort, based on its altitude coverage (up to 80 km) and implications for future geostationary  
229 satellite use. The system produces global, three-dimensional distributions of atmospheric composition  
230 with a spatial resolution of 25km. Using meteorological analyses from other GEOS systems, the GEOS-  
231 CF products include a running atmospheric replay to provide near-time estimates of surface pollutant  
232 distributions and the composition of the troposphere and stratosphere. Individual case study evaluations  
233 using ozone lidar of the GEOS-CF meteorological replay have recently been performed in Dacic *et al.*  
234 (2020), Gronoff *et al.* (2021) and Johnson *et al.* (2021). These results will also be used to better evaluate  
235 the GEOS-CF as the source of a priori ozone profiles for use in the TEMPO tropospheric ozone  
236 retrievals. Model output for this work is used from the closest GEOS-CF model grid cell to the CESAR  
237 observatory.

## 238 **3 Tropospheric Ozone Comparisons**

### 239 **3.1 Vertical Profiles**

240 Example tropospheric ozone profile observations are presented in **Figure 2** for 7 individual observation  
241 periods during the TROLIX-19 campaign. Each of the panels show the cloud screened TROPOZ lidar  
242 retrievals (top panels) and the corresponding GEOS-CF model output (bottom panels). Pink dots are  
243 overlaid to indicate the simulated tropopause altitude based on a blended estimate (TROPPB) which

244 meets criteria of the lowest altitude bin corresponding with either a pressure level above the thermal  
245 tropopause (380K) or dynamical (3 PVU) tropopause.

246 In general, the observations and simulations agree quite well in characterizing the broad features that  
247 impacted the CESAR site during the TROLIX-19 campaign. However, in each panel there are ozone  
248 laminae within the lower troposphere that are not replicated in the model simulation, most notably the  
249 underestimation of ozone during the September 20-21 period from 3-5km (Figure 2d-e). ~~The~~  
250 ~~observations indicate increased ozone levels as compared to the model during this period, centered~~  
251 ~~around the 3-5km and 8-10km region of the atmosphere (this is explored in more detail below, black~~  
252 ~~dashed box)~~. However, the model does simulate well the lowered tropopause height and abundance of  
253 lower stratospheric ozone observed in the 2 October observations (see Fig. 2g), which is an indication of  
254 the model ~~well representing the dynamical variability that affects the lowering of the tropopause~~  
255 ~~height~~ representing the dynamical variability that affects the lowering of the tropopause height. This  
256 suggests the model is appropriately capturing the complex dynamics during this period near the upper  
257 troposphere, but may not have been initialized with the correct boundary conditions or is too spatially  
258 coarse to allow for simulation of the layer emphasized with the black dashed box. However, this is an  
259 important altitude region for identifying long range transport of aged stratospheric air and inter-  
260 continental transport that may be downward mixing towards the surface layer and will be explored in  
261 more detail below.

262 To bring in additional platforms and to better understand these differences throughout the campaign at  
263 discrete altitudes, **Figure 3** shows the ozone number density values for the TROPOZ lidar, GEOS-CF  
264 model, TROPOMI and ECC ozonesondes at the average 4 km vertical level for the entire TROLIX-19  
265 campaign period. Within ~~the 4km~~ this layer, the platforms are all characterizing the general ozone  
266 features throughout the campaign at an altitude that frequently is associated with aged transported  
267 layering laminae. There is a noticeable difference between the observations and model during the  
268 previously described 20-21 September period. On 21 September at 12 UT, the lidar and ECC sonde

269 quantify an elevated layer ( $1.2-1.3 \times 10^{21}$  molecules  $m^{-3}$ ) -into the region that is not simulated by model  
270 ( $0.75-0.9 \times 10^{21}$  molecules  $m^{-3}$ ), resulting in an approximately 30% ~~difference in ozone abundance within~~  
271 ~~layer. Since the model correctly simulated many other ozone features during this time period within the~~  
272 ~~upper tropospheric region, this is likely aged transport into the domain that was not available during~~  
273 ~~model initialization. Back trajectories were performed to better identify the source of this air mass,~~  
274 ~~however nothing conclusive can be reported. The layer is not associated with any increase in lidar~~  
275 ~~attenuated backscatter within the associated altitude, suggesting it was not urban in origin and therefore~~  
276 ~~more likely aged stratospheric air mixing down to the lower free troposphere. Outside of this Sep 21~~  
277 ~~period, there is generally good agreement between the observations and model, indicating the~~  
278 ~~combination of observations and modeling are able to represent the rural conditions and ozone~~  
279 ~~perturbations at the CESAR site.~~underestimation in ozone abundance within the layer.

### 280 **3.2 Columnar Data Reduction**

281 There continues to be a need within the atmospheric and satellite community to understand the  
282 variability of ozone as it pertains to both the tropospheric column (*i.e.* the Earth's surface to the  
283 tropopause height) and the 0-2km tropospheric column (*i.e.* the Earth's surface to the 2 km height). The  
284 0-2 km region is of particular interest as it is projected to be delivered hourly from the North American  
285 geo-stationary satellite: Tropospheric Emissions: Monitoring of Pollution (TEMPO). Due to the  
286 increased temporal frequency and vertical extent of TEMPO's tropospheric ozone retrievals, ozone  
287 lidars, such as those from TOLNet (<https://www-air.larc.nasa.gov/missions/TOLNet/>) used in this work,  
288 are an ideal platform to perform future evaluations of the products, ~~which build from Johnson *et al.*,~~  
289 ~~2018.~~

290 Full tropospheric columns (**Figure 4, top panel**) are consistently calculated from each platform using  
291 the blended tropopause height (TROPPB) produced by the GEOS-CF and described above (*c.f.* pink dots  
292 in **Figure 2**) and are then converted to Dobson Units (DU). The tropospheric and 0-2km columns are

293 calculated explicitly by integrating the ozone number density from the lowest data bin of usable data to  
294 the TROPB or 2km layer height produced in the nearest model temporal output. The exception to this  
295 is the OMPS/MERRA-2 tropospheric column using the residual method described above (subtracting  
296 the MERRA-2 stratospheric column from the OMPS-NM total ozone column). ~~For the 0-2km~~  
297 ~~tropospheric column (Figure 4, bottom panel), there were no major surface layer pollution events at the~~  
298 ~~CESAR observatory during TROLIX-19.~~

299 For the full tropospheric column (Figure 4, top panel), the campaign variability ranges from  
300 approximately 20-55 DU; based on the lidar observations. The model, lidar, and ECC sonde  
301 observations agree quite well throughout the 12 Sep to 23 Sep time frame when looking at day-to-day  
302 variability. However, when assessing the variability on a single day for 21 Sep, full tropospheric  
303 columns reduced from the lidar observations are some of the largest observed during this TROLIX-19  
304 period (reaching nearly 5046 DU), while the but mostly staying between 34-40 DU. During this time,  
305 the model mainly ranges between 35-37 DU ~~or a difference, resulting in differences within 10% for~~  
306 ~~most of upwardsthe observations (albeit closer to 30% for the peak on this day).~~

307 When looking at Figure 2d-f, the lower ozone values just below the tropopause during this period are not  
308 simulated in the model, which may be an indication that the mesoscale ozone transport in the frontal  
309 system is not very well resolved by the model for this specific event. Since the model correctly  
310 simulated many other ozone features during this time period within the upper tropospheric region, this  
311 may also be attributed to aged transport into the domain that was not available during model  
312 initialization. Back-trajectories were performed to better identify the sources of 40%. Therefore, this  
313 these air masses, however nothing conclusive can be reported. The layer is not associated with any  
314 increase identified and discussed in Fig 3, not only results an in lidar attenuated backscatter within the  
315 associated altitude-specific difference, but ultimately results in a large overall impact to the full,  
316 suggesting it was not urban in origin and therefore more likely aged stratospheric air mixing down to the  
317 lower free troposphere. Outside of this Sep 21 period, there is generally good agreement between the

318 observations (including the OMPS-MERRA2 product) and model, indicating the combination of  
319 observations and modeling is able to represent the rural conditions and ozone perturbations at the  
320 CESAR site.

321 When assessing these tropospheric column values from the TROPOMI ozone profile  
322 observations, it is important to mention the vastly different vertical resolution or averaging kernel  
323 schemes as compared to the independent observations near the tropopause. The ECC samples an  
324 instantaneous observation with a vertical resolution generally less than 100m, while the lidar is  
325 averaging over 500-750m of atmosphere for each data point near the tropopause. However, the vertical  
326 resolution near the tropopause for TROPOMI using the TOPAS algorithm (Mettig *et al.*, 2021) is nearly  
327 6 km, indicating it is not able to completely represent sharp gradients that may occur near the tropopause  
328 layer and the lower stratosphere (where ozone content sharply increases). This lack of degrees of  
329 independent information is evident in the relatively higher TROPOMI tropospheric column ozone values  
330 as compared to the other independent measurements presented in this work. This suggests ground-based  
331 profiling observations are still critically needed to confirm large deviations from a priori and  
332 climatology in order to evaluate the atmospheric chemistry models, especially in the upper tropospheric  
333 region and within the boundary layer.

334 There exists both diurnal and day-to-day variability of the 0-2 km ozone, ranging from 4-10 DU (Figure  
335 4, ~~top~~bottom panel). In the 0-2 km ozone reduction, the lidar and model are critically needed to  
336 understand ozone variability on a continuous scale. For instance, on 15 Sep the 0-2 km ozone column  
337 was near 9 DU at 03 UT and finished near 5.5 DU at 16 UT, resulting in a -60% change in DU within a  
338 ~~single day. Furthermore, the gradient of the 21 Sep ozone column change was similar in scale to the~~  
339 ~~entire campaign variability, indicating that there is a significant amount of information gained in the~~  
340 ~~understanding of the variability in ozone from continuous measurements. Although a daily snapshot of~~  
341 ~~OMPS-MERRA-2 residuals and TROPOMI ozone profile observations are critical for their vast spatial~~  
342 ~~coverage, ground-based observations such as ozone lidar and ECC sondes are critically needed to~~

343 ~~quantify measurement gaps.~~ 13 hours. The need for continuous measurements during highly variable  
344 days are further emphasized by the fact that this gradient in 0-2km ozone for this single day (15 Sep, 5.5  
345 DU – 9 DU) was comparable to the variance of 0-2 km ozone values throughout the entire campaign.  
346 In summary, we find that the ozone columns evaluated in this study generally reproduced the structure  
347 of the TROLIX-19 ozone lidar observations for N=835 coincidences. For the full tropospheric column,  
348 the lidar calculated median was  $30.9 \pm 4.7$  DU, compared to  $33.4 \pm 3.9$  DU for the GEOS-CF. This  
349 indicates a difference of 2.5 DU or 7.9 %, which is well within the lidar uncertainty of around 10 %  
350 throughout the tropospheric column, and as we described above is likely driven by select days rather  
351 than an overall bias between the measurements. For the 0-2 km tropospheric column, the lidar  
352 calculated median was  $5.8 \text{ DU} \pm 0.9 \text{ DU}$ , compared to ~~6.9~~7.8  $\text{DU} \pm 0.7 \text{ DU}$  for the corresponding  
353 GEOS-CF measurements. ~~This indicates a difference between observations and model of 1.1 DU or 18.9~~  
354 ~~%, which is higher than the lidar uncertainty of around 5–10 % throughout the column.~~ For the  
355 TROLIX-19 campaign, a 0-2 km tropospheric column accounts for approximately 20% of the  
356 tropospheric column as detailed in Figure 4 (top panel), indicating measurements above the surface are  
357 critically needed at understanding ozone variability at rural sites such as Cabauw, NL, where free  
358 tropospheric ozone features dominate the column.

## 359 **4 Full Profile Ozone Comparisons**

### 360 **4.1 Hybrid Tropospheric/Stratospheric Ozone Comparisons**

361 To better understand differences in ozone retrievals from multiple platforms, it is important to assess the  
362 entire vertical distribution of ozone. To characterize the vertical distribution throughout the entire  
363 troposphere and stratosphere, hybrid ozone profiles were created from longer (integrations of 60-120  
364 ~~minute~~minutes vs 10 minutes in Sec 3) temporal retrievals from the closed co-located daytime/nighttime  
365 TROPOZ and nighttime STROZ ~~lidar~~lidar data, which were then interpolated to the GEOS-CF model  
366 vertical grid levels. **Figure 5** compares these results to the GEOS-CF, OMPS-LP, TROPOMI, MLS and

367 the ECC ozonesonde profiles for 12 Sep, 17 Sep, 19 Sep, and 21 Sep 2019. These days were selected as  
368 days within the campaign that had an ECC launch from De Bilt, NL (30 km from Cabauw).  
369 For each observation period in **Figure 5**, all platforms manage to characterize a similar shape and extent  
370 of the ozone maxima between 2.5-4.5 molecules m<sup>-3</sup> throughout the vertical layer between 20-25 km. In  
371 each case, there are differences between the platforms in characterizing the vertical variability and  
372 extent of the ozone maxima, which will be quantified in the following section. One notable feature that  
373 emphasizes the cross-platform ability to illustrate ozone variability in the stratosphere is from the 19 and  
374 21 Sep profiles. A dual ozone maximum is observed quite remarkably by the merged lidar, ECC, MLS,  
375 OMPS-LP and simulated by the GEOS-CF centered around 20 km and then again at 25km. The wind  
376 observations from the ozonesonde payload (not shown) indicate a wind shear within the two ozone  
377 layers, suggesting this feature was dynamically driven. The TROPOMI retrieval is not able to retrieve  
378 this vertical features due to its coarser vertical resolution and appears to average through the layers.

#### 379 **4.2 Difference Profiles**

380 To quantitatively compare the ozone retrievals and simulations, **Figure 6** displays the ozone  
381 values for the TROLIX-19 time period from the hybrid lidar dataset (**Figure 6a**), GEOS-CF (**Figure**  
382 **6b**), OMPS-LP (**Figure 6c**), MLS (**Figure 6d**) and TROPOMI (**Figure 6e**). This double ozone maxima,  
383 starting after 20 September serves as a geophysical marker to visually compare the ozone products. The  
384 lidar, model, and OMPS-LP all capture this feature, but with varying ozone abundances and altitudes.  
385 From **Figure 6d**, it appears as if TROPOMI retrievals are not able to resolve this feature. The percent  
386 differences, as compared to the lidar observations, are displayed in **Figure 7a-d**. These percent  
387 differences are calculated using (1)

$$(1) \text{ Percent Difference} = \frac{(E_1 - E_2)}{\frac{1}{2}(E_1 + E_2)} \times 100$$

390  
391



392 where  $E_2$  are the lidar observations and  $E_1$  are the respective ozone values from the various platforms in  
393 **Figure 6**.

394 The percent differences in **Figure 7a** indicate the GEOS-CF model from 20-45 km generally represents  
395 the lidar observations, but are generally 0-10 % lower in abundance. The percent differences in **Figure**  
396 **7b** indicate OMPS-LP is also representing the ozone maxima and altitude above 25 km. There are larger  
397 differences below 20 km, which indicates the OMPS-LP retrieval ~~is generally underestimating~~  
398 ~~how~~ worsens (in both directions) as compared to the ozone abundance below 20 km as shown in the  
399 profiles in **Figure 5**. The percent differences in **Figure 7c** indicate the MLS data, especially that within  
400 the 20-40km region, perform quite well as compared to the lidar observations. The percent differences in  
401 **Figure 7d** indicate the TROPOMI retrieval is generally over representing the ozone concentrations  
402 throughout the atmosphere, which worsens within the troposphere- and has been discussed earlier for  
403 the tropospheric ozone column as a result of a much larger vertical resolution in this region. In all cases,  
404 the most variability in the differences occur within the active region from 10-20 km that is driven by the  
405 dynamical tropopause height and lower stratospheric ozone abundance. Within each satellite dataset, we  
406 find larger biases in the lower stratosphere and upper troposphere below 18km, which has been  
407 previously described in the literature for the OMPS-LP dataset in Kramarova *et al.*, 2018 and were  
408 improved in the updated version 2.5 algorithm used in this work.

## 409 **5 Total Column Ozone**

410 Similar to the troposphere, to better understand to what extent the vertical distribution of ozone impacts  
411 the atmospheric column, **Figure 8 (top panel)** shows the various platforms and their retrieved total  
412 column ozone. For this analysis, the GEOS-CF, lidar, OMPS-NM, TROPOMI (GODFIT) are shown, in  
413 addition to local ground-based measurements from a Pandora instrument and Brewer. The total column  
414 values range from 230-300 DU throughout the campaign period, with the median total column ozone of  
415 271 DU. With the previous analyses from Sec 3.2, this indicates the median total tropospheric column of

416 33 DU and 0-2km boundary layer column of 6 DU result in percentages of the entire ozone column of  
417 12% and 2.3%, respectively. Similar to the full tropospheric ozone columns, larger total ozone columns  
418 were observed towards the end of the TROLIX-19 period, suggesting this variability was partly due to a  
419 larger abundance of ozone in the lower stratosphere.

420 **Figure 8 (bottom panel)** shows the various platforms as a percent differences from the model. In  
421 general, the various platforms are all mostly within ±05 % of each other, with most differences being  
422 within ±53%. This analysis emphasizes the stability and maturity of the Pandora and Brewer systems for  
423 monitoring the total column ozone amounts. Interestingly, the double maxima feature in vertical ozone  
424 distribution in the stratosphere (with local minima between) described in Sec 4.1 on 21 Sep does not  
425 severely impact the total column ozone.

## 426 **6 Conclusions**

427 This work has highlighted the various differences in retrieved ozone quantities during the TROLIX-19  
428 campaign. This has emphasized the importance of ground-based ozone lidars and other measurements in  
429 understanding the vertical variability of ozone and how it relates to the column reduction. This work  
430 also shows the first effort to directly resolve both tropospheric columns and 0-2km ozone columns from  
431 the NASA TROPOZ lidar. Other TOLNet lidars are able to perform this data reduction and future work  
432 will be to expand this effort to the other TOLNet locations. This work indicates the level of performance  
433 of the GEOS-CF modeling system as compared to the other platforms, which ultimately performs  
434 extremely well both in the stratosphere (Figure 6 and Figure 7) and within the troposphere, ~~as~~  
435 emphasized (Figure 2 and Figure 4).

436 One takeaway message or point of caution for future efforts is that although there are situations  
437 identified where the vertical profile and the model disagree in Figure 6 and Figure 7, a certain altitude  
438 range (Figure 3), when the data is reduced to a columnar product, compensating over/under-estimations  
439 may cancel out and produce a more accurate value when only looking at the resultant as compared to

440 observations. For this reason, it is essential when doing data columnar reduction for the troposphere, and  
441 even more so in the 0-2km column or planetary boundary layer, that observations of the vertical profile  
442 be used to evaluate the representativeness of the model and auxillary data sets.

443 In looking towards the NASA TEMPO ~~mission~~, this work indicates that the GEOS-CF, with its global  
444 coverage, hourly resolution, and adequate vertical information to resolve most atmospheric features, is  
445 an appropriate choice for the a priori profiles for the TEMPO ozone retrievals. Continued investigations  
446 are needed with high resolution observations, as presented in this work, to better evaluate the GEOS-CF,  
447 especially in these common transport regions of the atmosphere. Although the GEOS-CF performed  
448 well in reproducing the ozone downward transport throughout the upper troposphere and lower  
449 stratosphere, the model did fail to resolve some high-resolution laminae deeper into the lower  
450 troposphere related to specific mesoscale ozone transport in this region as evidenced in Figure 2 and  
451 Figure 3.

452 This work shows the TROPOMI TOPAS ozone profile algorithm products are able to accurately  
453 reproduce ozone quantities in the lower troposphere at various atmospheric levels. In particular, **Figure**  
454 **3** shows and Figure 4 show promising results that indicate the TROPOMI satellite observations compare  
455 well with the observations from ground-based measurements (lidar, sonde) of specific elevated ozone  
456 features. However, there is an observed overestimate of the TROPOMI retrieval in the upper  
457 troposphere and lower stratosphere (between 10 and 15 km) associated with a larger vertical resolution  
458 that needs to also be further evaluated to better understand the representativeness of the retrieval in this  
459 region.

460  
461 Figure 7 was presented as a quantitative resultant figure to illustrate both the temporal (*i.e.*, throughout  
462 the course of the TROLIX-19 campaign) and vertical differences observed in the retrievals from each  
463 observational platform. This serves as a rare opportunity to cross-evaluate multiple satellited based  
464 observations, a global chemical transport model, ozonesondes and a high-resolution ozone lidar suite.

465 The authors feel that this figure has served to point out the strengths of each platform and present careful  
466 considerations for areas of under/over estimation, Furthermore, we feel reducing these comparisons  
467 down to a specific percentage may underserve the community push for supporting the vertical profiling  
468 needed for these types of efforts.

469 The CESAR Observatory continues to be a critical landmark for campaigns that revolve around  
470 atmospheric composition measurements for satellite validation and evaluation beyond this effort, such as  
471 CINDI and CINDI-2 (Kreher *et al.*, [2020](#); Wang *et al.*, 2020; Tirpitz *et al.*, 2021). As the European  
472 Commission (EC) in partnership with the European Space Agency (ESA) continues to launch  
473 tropospheric composition satellites, including the upcoming geo-stationary Sentinel-4 satellite, we  
474 expect this observatory will continue to host and maintain critical atmospheric sampling for future  
475 validation efforts.

476

477

478

#### 479 **Data Availability.**

480

481 1. MLS ozone profiles can be downloaded from the NASA Goddard Space Flight Center Earth  
482 Sciences Data and Information Services Center (GES DISC; Schwartz *et al.*, 2020,  
483 <https://doi.org/10.5067/Aura/MLS/DATA2516>, last access: 29 March 2022).

484 2. The Pandora data is available at the Pandonia Global Network Archive ( [http://data.pandonia-](http://data.pandonia-global-network.org/Cabauw/)  
485 [global-network.org/Cabauw/](http://data.pandonia-global-network.org/Cabauw/), last access 29 March 29, 2022).

486 3. The OMPS LP version 2.5 ozone profiles can be downloaded from the NASA Goddard Space  
487 Flight Center Earth Sciences Data and Information Services Center (GES DISC;  
488 at <https://doi.org/10.5067/X1Q9VA07QDS7> (Deland, 2017, last access: 29 March 2022).

489 4. The tropospheric ozone lidar data used in this publication were obtained from the Cabauw  
490 Experimental Site for Atmospheric Research (CESAR) as part of a campaign involving the

491 Network for the Detection of Atmospheric Composition Change (NDACC) and NASA's  
492 Tropospheric Ozone Lidar Network (TOLNet) and are publicly available ([https://www-  
493 air.larc.nasa.gov/cgi-bin/ArcView.1/TOLNet?NASA-GSFC=1](https://www-air.larc.nasa.gov/cgi-bin/ArcView.1/TOLNet?NASA-GSFC=1), last access: 29 March 2022).

494 5. The ozonesonde and Brewer data used in this publication were obtained from the De Bilt, NL  
495 site as part of a campaign involving the Network for the Detection of Atmospheric Composition  
496 Change (NDACC) and are publicly available (<ftp://ftp.cpc.ncep.noaa.gov/ndacc/station/debilt/>,  
497 last access: 29 March 2022).

498 6. The stratospheric ozone lidar data used in this publication were obtained from the Cabauw  
499 Experimental Site for Atmospheric Research (CESAR) as part of a campaign involving the  
500 Network for the Detection of Atmospheric Composition Change (NDACC) and are publicly  
501 available (<ftp://ftp.cpc.ncep.noaa.gov/ndacc/station/cabauw/>, last access: 29 March 2022).

502 7. The TROPOMI TOPAS Ozone Profile data and source codes are available upon request from  
503 Nora Mettig ([mettig@iup.physik.uni-bremen.de](mailto:mettig@iup.physik.uni-bremen.de)) or Mark Weber ([weber@uni-bremen.de](mailto:weber@uni-bremen.de)). The  
504 L1B version of the S5P data is available upon request to the S5P Validation Team.

505 8. The Tropospheric Ozone Column from OMPS-NM/MERRA-2 Daily measurements data are  
506 available upon request from Jerry Ziemke ([Jerald.r.ziemke@nasa.gov](mailto:Jerald.r.ziemke@nasa.gov)).

507 9. The NASA GEOS-CF simulations are available at the data sharing portal  
508 (<https://portal.nccs.nasa.gov/datashare/gmao/geos-cf/v1/forecast/>, last access 29 March 2022).

509

510 Author contributions. JS drafted the original manuscript. JS, LT, GS, and TM deployed and operated the  
511 NASA ozone lidars and provided expertise on use of measurements. NM, AR, and MW provided  
512 TOPAS ozone profile data and guidance on how best to use the measurements. AA and KK provided  
513 overall context as principal investigators of the TROLIX-19 campaign and coordinated science team  
514 meetings to foster this collaboration. KEK provided GEOS-CF data and insight on its use in this work.  
515 MA, AP, MvR, and PV provided expertise and data for the ground-observations for ozonesondes,

516 Brewer, and historical data for the Cabauw site. JZ provided data for the OMPS-MERRA-2 tropospheric  
517 column data. NK provided Aura MLS, OMPS-LP merged data and further insight into the use of the  
518 data.

519

520

521 Competing interests. The authors declare that they have no conflict of interest.

522

523 Disclaimer. Publisher's note: Copernicus Publications remains neutral with regard to jurisdictional  
524 claims in published maps and institutional affiliations.

525

526 Acknowledgements. NASA data has been provided through the Tropospheric Composition and Upper  
527 Atmosphere Research Programs. We acknowledge all additional data providers and their funding  
528 agencies for performing regular measurements and retrievals.

529

530

531

532

533

534

535

536

537

538

539

540

541

542

543

544

545

546

547

548

549

550

552 **References**

553

554 Apituley, Arnoud, Karin Kreher, Michael Van Roozendaal, John Sullivan, Thomas J. McGee, Marc  
 555 Allaart, Ankie PETERS et al. "Overview of activities during the 2019 TROPOMI validation experiment  
 556 (TROLIX'19)." In *AGU Fall Meeting Abstracts*, vol. 2019, pp. A43J-2958. 2019

557

558 Apituley, Arnoud, Karin Kreher, Ankie PETERS, John Sullivan, Michel van Roozendaal, Tim Vlemmix,  
 559 Mirjam den Hoed et al. "Overview of the 2019 Sentinel-5P TROPOMI validation experiment  
 560 (TROLIX)." In *EGU General Assembly Conference Abstracts*, p. 10539. 2020.

561

562 Arosio, Carlo, Alexei Rozanov, Elizaveta Malinina, Kai-Uwe Eichmann, Thomas von Clarmann, and  
 563 John P. Burrows. "Retrieval of ozone profiles from OMPS limb scattering observations." *Atmospheric  
 564 Measurement Techniques* 11, no. 4 (2018): 2135-2149.

565

566 Copernicus Sentinel data processed by ESA, German Aerospace Center (DLR) (2019), Sentinel-5P  
 567 TROPOMI Total Ozone Column 1-Orbit L2 5.5km x 3.5km, Greenbelt, MD, USA, Goddard Earth  
 568 Sciences Data and Information Services Center (GES DISC), Accessed: [10 December 2021],  
 569 [10.5270/S5P-fqouvyz](https://doi.org/10.5270/S5P-fqouvyz)

570

571 Dacic, Natasha, John T. Sullivan, K. Emma Knowland, Glenn M. Wolfe, Luke D. Oman, Timothy A.  
 572 Berkoff, and Guillaume P. Gronoff. "Evaluation of NASA's high-resolution global composition  
 573 simulations: Understanding a pollution event in the Chesapeake Bay during the summer 2017 OWLETS  
 574 campaign." *Atmospheric Environment* 222 (2020): 117133.

575

576 [Flynn, L. E., Seftor, C. J., Larsen, J. C., and Xu, P.: The Ozone Mapping and Profiler Suite, in: Earth  
 577 Science Satellite Remote Sensing, edited by: Qu, J. J., Gao, W., Kafatos, M., Murphy, R. E., and  
 578 Salomonson, V. V., Springer, Berlin, 279–296, doi:10.1007/978-3-540-37293-6, 2006.](#)

579

580 Garane, Katerina, Maria-Elissavet Koukouli, Tjil Verhoelst, Christophe Lerot, Klaus-Peter Heue, Vitali  
 581 Fioletov, Dimitrios Balis et al. "TROPOMI/S5P total ozone column data: global ground-based  
 582 validation and consistency with other satellite missions." *Atmospheric Measurement Techniques* 12, no.  
 583 10 (2019): 5263-5287.

584

585 Gronoff, G., T. Berkoff, K. E. Knowland, L. Lei, M. Shook, B. Fabbri, W. Carrion, and A. O. Langford.  
 586 "Case study of stratospheric intrusion above Hampton, Virginia: lidar-observation and modeling  
 587 analysis." *Atmospheric Environment* (2021): 118498.

588

589 Hubert, Daan, Klaus-Peter Heue, Jean-Christopher Lambert, Tjil Verhoelst, Marc Allaart, Steven  
 590 Compennolle, Patrick D. Cullis et al. "TROPOMI tropospheric ozone column data: geophysical  
 591 assessment and comparison to ozonesondes, GOME-2B and OMI." *Atmospheric Measurement  
 592 Techniques* 14, no. 12 (2021): 7405-7433.

593

594 Johnson, M. S., Liu, X., Zoogman, P., Sullivan, J., Newchurch, M. J., Kuang, S., Leblanc, T., and  
 595 McGee, T.: Evaluation of potential sources of a priori ozone profiles for TEMPO tropospheric ozone  
 596 retrievals, *Atmos. Meas. Tech.*, 11, 3457–3477, <https://doi.org/10.5194/amt-11-3457-2018>, 2018.

597

598 Keller, Christoph A., K. Emma Knowland, Bryan N. Duncan, Junhua Liu, Daniel C. Anderson, Sampa  
599 Das, Robert A. Lucchesi et al. "Description of the NASA GEOS Composition Forecast Modeling  
600 System GEOS-CF v1. 0." *Journal of Advances in Modeling Earth Systems* 13, no. 4 (2021):  
601 e2020MS002413.  
602

603 Kramarova, Natalya A., Pawan K. Bhartia, Glen Jaross, Leslie Moy, Philippe Xu, Zhong Chen, Matthew  
604 DeLand et al. "Validation of ozone profile retrievals derived from the OMPS LP version 2.5 algorithm  
605 against correlative satellite measurements." *Atmospheric Measurement Techniques* 11, no. 5 (2018):  
606 2837-2861.  
607

608 Kreher, Karin, Michel Van Roozendaal, Francois Hendrick, Arnoud Apituley, Ermioni Dimitropoulou,  
609 Udo Frieß, Andreas Richter et al. "Intercomparison of NO<sub>2</sub>, O<sub>4</sub>, O<sub>3</sub> and HCHO slant column  
610 measurements by MAX-DOAS and zenith-sky UV–visible spectrometers during CINDI-2."  
611 *Atmospheric Measurement Techniques* 13, no. 5 (2020): 2169-2208.  
612

613 Lamsal, L. N., M. Weber, S. Tellmann, and J. P. Burrows. "Ozone column classified climatology of  
614 ozone and temperature profiles based on ozonesonde and satellite data." *Journal of Geophysical*  
615 *Research: Atmospheres* 109, no. D20 (2004).  
616

617 Leblanc, Thierry, Mark A. Brewer, Patrick S. Wang, Maria Jose Granados-Muñoz, Kevin B.  
618 Strawbridge, Michael Travis, Bernard Firanski et al. "Validation of the TOLNet lidars: the Southern  
619 California Ozone Observation Project (SCOOP)." *Atmospheric measurement techniques* 11, no. 11  
620 (2018): 6137-6162.  
621

622 [Leblanc, Thierry, Robert J. Sica, Joanna AE Van Gijssel, Sophie Godin-Beekmann, Alexander Haefele,](#)  
623 [Thomas Trickl, Guillaume Payen, and Gianluigi Liberti. "Proposed standardized definitions for vertical](#)  
624 [resolution and uncertainty in the NDACC lidar ozone and temperature algorithms–Part 2: Ozone DIAL](#)  
625 [uncertainty budget." \*Atmospheric Measurement Techniques\* 9, no. 8 \(2016\): 4051-4078.](#)  
626

627 Livesey, N. J., M. J. Filipiak, L. Froidevaux, W. G. Read, A. Lambert, M. L. Santee, J. H. Jiang et al.  
628 "Validation of Aura Microwave Limb Sounder O<sub>3</sub> and CO observations in the upper troposphere and  
629 lower stratosphere." *Journal of Geophysical Research: Atmospheres* 113, no. D15 (2008).  
630

631 Malderen, Roeland Van, Marc AF Allaart, Hugo De Backer, Herman GJ Smit, and Dirk De Muer. "On  
632 instrumental errors and related correction strategies of ozonesondes: possible effect on calculated ozone  
633 trends for the nearby sites Uccle and De Bilt." *Atmospheric Measurement Techniques* 9, no. 8 (2016):  
634 3793-3816.  
635

636 McGee, Thomas J., David N. Whiteman, Richard A. Ferrare, James J. Butler, and John F. Burris.  
637 "STROZ LITE: stratospheric ozone lidar trailer experiment." *Optical Engineering* 30, no. 1 (1991): 31-  
638 39.  
639

640 McPeters, Richard D., Gordon J. Labow, and Jennifer A. Logan. "Ozone climatological profiles for  
641 satellite retrieval algorithms." *Journal of Geophysical Research: Atmospheres* 112, no. D5 (2007).  
642

643 Mettig, N., Weber, M., Rozanov, A., Arosio, C., Burrows, J. P., Veefkind, P., Thompson, A. M., Querel,  
644 R., Leblanc, T., Godin-Beekmann, S., Kivi, R., and Tully, M. B.: Ozone profile retrieval from nadir  
645 TROPOMI measurements in the UV range, *Atmos. Meas. Tech.*, 14, 6057–6082,  
646 <https://doi.org/10.5194/amt-14-6057-2021>, 2021.  
647



648 Mettig, Nora, Mark Weber, Alexei Rozanov, John P. Burrows, Pepijn Veefkind, Nadia Smith, Anne M.  
649 Thompson et al. "Combined UV and IR ozone profile retrieval from TROPOMI and CrIS  
650 measurements." *Atmospheric Measurement Techniques Discussions* (2021): 1-33.  
651

652 Peters, A. J. M., Boersma, K. F., Kroon, M., Hains, J. C., Van Roozendaal, M., Wittrock, F., Abuhassan,  
653 N., Adams, C., Akrami, M., Allaart, M. A. F., Apituley, A., Beirle, S., Bergwerff, J. B., Berkhout, A. J.  
654 C., Brunner, D., Cede, A., Chong, J., Clémer, K., Fayt, C., Frieß, U., Gast, L. F. L., Gil-Ojeda, M.,  
655 Goutail, F., Graves, R., Griesfeller, A., Großmann, K., Hemerijckx, G., Hendrick, F., Henzing, B.,  
656 Herman, J., Hermans, C., Hoexum, M., van der Hoff, G. R., Irie, H., Johnston, P. V., Kanaya, Y., Kim,  
657 Y. J., Klein Baltink, H., Kreher, K., de Leeuw, G., Leigh, R., Merlaud, A., Moerman, M. M., Monks, P.  
658 S., Mount, G. H., Navarro-Comas, M., Oetjen, H., Pazmino, A., Perez-Camacho, M., Peters, E., du  
659 Piesanie, A., Pinardi, G., Puentedura, O., Richter, A., Roscoe, H. K., Schönhardt, A., Schwarzenbach,  
660 B., Shaiganfar, R., Sluis, W., Spinei, E., Stolk, A. P., Strong, K., Swart, D. P. J., Takashima, H.,  
661 Vlemmix, T., Vrekoussis, M., Wagner, T., Whyte, C., Wilson, K. M., Yela, M., Yilmaz, S., Zieger, P.,  
662 and Zhou, Y.: The Cabauw Intercomparison campaign for Nitrogen Dioxide measuring Instruments  
663 (CINDI): design, execution, and early results, *Atmos. Meas. Tech.*, 5, 457–485, doi:10.5194/amt-5-457-  
664 2012, 2012.  
665

666 [Smit, H. G. J., Thompson, A. M., & the Panel for the Assessment of Standard Operating Procedures for](#)  
667 [Ozonesondes, v2.0 \(ASOPOS 2.0\) \(2021\). Ozonesonde Measurement Principles and Best Operational](#)  
668 [Practices. World Meteorological Organization, GAW Report 268. \[Available](#)  
669 [at https://library.wmo.int/doc\\_num.php?explnum\\_id=10884](https://library.wmo.int/doc_num.php?explnum_id=10884).  
670

671 [Smit, Herman GJ, Wolfgang Straeter, Bryan J. Johnson, Samuel J. Oltmans, Jonathan Davies, David](#)  
672 [W. Tarasick, Bruno Hoegger et al. "Assessment of the performance of ECC-ozonesondes under quasi-](#)  
673 [flight conditions in the environmental simulation chamber: Insights from the Juelich Ozone Sonde](#)  
674 [Intercomparison Experiment \(JOSIE\)." \*Journal of Geophysical Research: Atmospheres\* 112, no. D19](#)  
675 [\(2007\)](#).  
676

677 Sullivan, J. T., T. J. McGee, G. K. Sumnicht, L. W. Twigg, and R. M. Hoff. "A mobile differential  
678 absorption lidar to measure sub-hourly fluctuation of tropospheric ozone profiles in the Baltimore–  
679 Washington, DC region." *Atmospheric Measurement Techniques* 7, no. 10 (2014): 3529-3548.  
680

681 Sullivan, John T., Thomas J. McGee, Anne M. Thompson, R. Bradley Pierce, Grant K. Sumnicht,  
682 Laurence W. Twigg, Edwin Eloranta, and Raymond M. Hoff. "Characterizing the lifetime and  
683 occurrence of stratospheric-tropospheric exchange events in the rocky mountain region using high-  
684 resolution ozone measurements." *Journal of Geophysical Research: Atmospheres* 120, no. 24 (2015):  
685 12410-12424.  
686

687 Sullivan, John T., Timothy Berkoff, Guillaume Gronoff, Travis Knepp, Margaret Pippin, Danette Allen,  
688 Laurence Twigg et al. "The ozone water–land environmental transition study: An innovative strategy for  
689 understanding Chesapeake Bay pollution events." *Bulletin of the American Meteorological Society* 100,  
690 no. 2 (2019): 291-306.  
691

692 Tirpitz, Jan-Lukas, Udo Frieß, François Hendrick, Carlos Alberti, Marc Allaart, Arnoud Apituley, Alkis  
693 Bais et al. "Intercomparison of MAX-DOAS vertical profile retrieval algorithms: studies on field data  
694 from the CINDI-2 campaign." *Atmospheric Measurement Techniques* 14, no. 1 (2021): 1-35.  
695

696 [van Geffen, J.H.G.M., Eskes, H.J., Boersma, K.F., Maasakkers, J.D. and Veeffkind, J.P., TROPOMI](#)  
697 [ATBD of the total and tropospheric NO2 data products, Report S5P-KNMI-L2-0005-RP, KNMI, De](#)  
698 [Bilt, The Netherlands; see TROPOMI ATBD list for the latest available version.](#)  
699  
700 [Wang, Yang, Arnoud Apituley, Alkiviadis Bais, Steffen Beirle, Nuria Benavent, Alexander Borovski,](#)  
701 [Ilya Bruchkouski et al. "Inter-comparison of MAX-DOAS measurements of tropospheric HONO slant](#)  
702 [column densities and vertical profiles during the CINDI-2 campaign." \*Atmospheric Measurement\*](#)  
703 [\*Techniques\* 13, no. 9 \(2020\): 5087-5116.](#)  
704  
705 Wenig, Mark O., A. M. Cede, E. J. Bucsela, E. A. Celarier, K. F. Boersma, J. P. Veeffkind, E. J.  
706 Brinksma, J. F. Gleason, and J. R. Herman. "Validation of OMI tropospheric NO2 column densities  
707 using direct-Sun mode Brewer measurements at NASA Goddard Space Flight Center." *Journal of*  
708 *Geophysical Research: Atmospheres* 113, no. D16 (2008).  
709  
710 Wing, Robin, Wolfgang Steinbrecht, Sophie Godin-Beekmann, Thomas J. McGee, John T. Sullivan,  
711 Grant Sumnicht, Gérard Ancellet, Alain Hauchecorne, Sergey Khaykin, and Philippe Keckhut.  
712 "Intercomparison and evaluation of ground-and satellite-based stratospheric ozone and temperature  
713 profiles above Observatoire de Haute-Provence during the Lidar Validation NDACC Experiment  
714 (LAVANDE)." *Atmospheric Measurement Techniques* 13, no. 10 (2020): 5621-5642.  
715  
716 Wing, Robin, Sophie Godin-Beekmann, Wolfgang Steinbrecht, Thomas J. Mcgee, John T. Sullivan,  
717 Sergey Khaykin, Grant Sumnicht, and Laurence Twigg. "Evaluation of the new DWD ozone and  
718 temperature lidar during the Hohenpeißenberg Ozone Profiling Study (HOPS) and comparison of results  
719 with previous NDACC campaigns." *Atmospheric Measurement Techniques* 14, no. 5 (2021): 3773-3794.  
720  
721 Ziemke, Jerry R., Luke D. Oman, Sarah A. Strode, Anne R. Douglass, Mark A. Olsen, Richard D.  
722 McPeters, Pawan K. Bhartia et al. "Trends in global tropospheric ozone inferred from a composite  
723 record of TOMS/OMI/MLS/OMPS satellite measurements and the MERRA-2 GMI simulation."  
724 *Atmospheric Chemistry and Physics* 19, no. 5 (2019): 3257-3269.  
725  
726  
727  
728  
729  
730  
731  
732  
733  
734  
735  
736  
737  
738  
739  
740  
741  
742  
743  
744  
745

746  
747  
748  
749  
750  
751  
752  
753

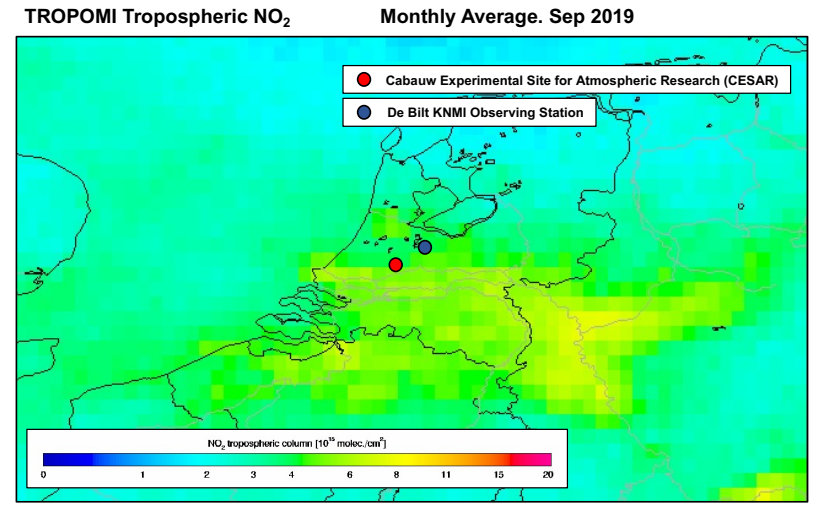
754 **Table 1: Instrument platforms, associated products, and short description used in this work during the TROLIX-19**  
755 **campaign.**

756

Instrument	Products	Platform	Description
GSFC TROPOZ [NASA]	Profiles [0.2 – 18 km]	Ground-based Lidar	10 min integration; 30-90-min avg around ECC or Satellite Overpass
GSFC STROZ [NASA]	Profiles [15 - 48 km]	Ground-based Lidar	~2-4-hr avg between (20-23 UT)
ECC Ozonesondes [KNMI]	Profiles [0 – 33 km]	Balloonborne	Balloonborne, Launched at 12 UT from De Bilt (~30 km from Cabauw) on 4 days
Pandora [NASA/KNMI]	Column [TCO]	Spectrometer	L2 Pandora 118s, Data Used has QC/QA Flags = 10
Brewer [KNM]	Column [TCO]	Spectrophotometer	L2 Brewer #189m, MKIII, Located in De Bilt
S5P/TropOMI [ESA]	Column [TCL]	Satellite	L2 TOPAS Product, Overpass between 12-14 UT (5.5x3.5 km, nadir)
S5P/TropOMI [KNMI]	Column [TCO]	Satellite	L2 GODFIT v4 TO3 Product, Overpass between 12-14 UT (5.5x3.5 km, nadir)
OMPS [NASA]	Column [TCO]	Satellite	L3 NM Product, Version 2, Daily Overpass between 12-14 UT (50x50 km, nadir)
OMPS-LP [NASA]	Profiles [12-60km]	Satellite	Merged L2 v2.5 Daily Merged Product, Overpass between 12-14 UT (1km vertical bins)
OMPS/MERRA-2 [NASA]	Trop. Columns	Satellite/Assimilation	L4 Derived Product, OMPS-NM daily Overpass, MERRA-2
AURA MLS [NASA]	Profiles [12-60km]	Satellite	Merged L2 v5 Daily Daytime/Nighttime Products, Overpass between 12-14 UT (1km vertical bins) and 01-03 UT.
GEOS-CF [NASA]	Profiles [0-80km]	Global 3-D CCMM	<u><a href="https://gmao.gsfc.nasa.gov/weather_prediction/GEOS-CF/">1-Hr, 72 lev, Met. Replay, (25x25km)</a></u>

757

758  
759  
760  
761  
762  
763  
764  
765  
766  
767

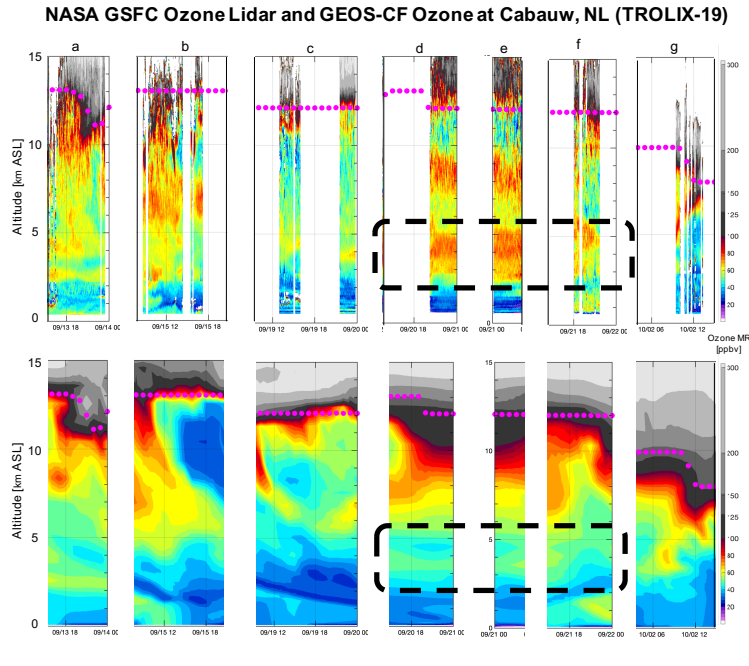


768  
769  
770

771 **Figure 1: ~~Aqua/MODIS True Color Corrected Reflectance (left) and TROPOMI Tropospheric~~ monthly-mean**  
772 **tropospheric NO<sub>2</sub> (right column (version 1.0)) for 14-September 2019. The CESAR site is and De Bilt, NL sites are**  
773 **indicated in the image on the left.**

774  
775  
776  
777  
778  
779  
780  
781  
782  
783  
784  
785  
786  
787  
788  
789

790  
791  
792  
793  
794  
795

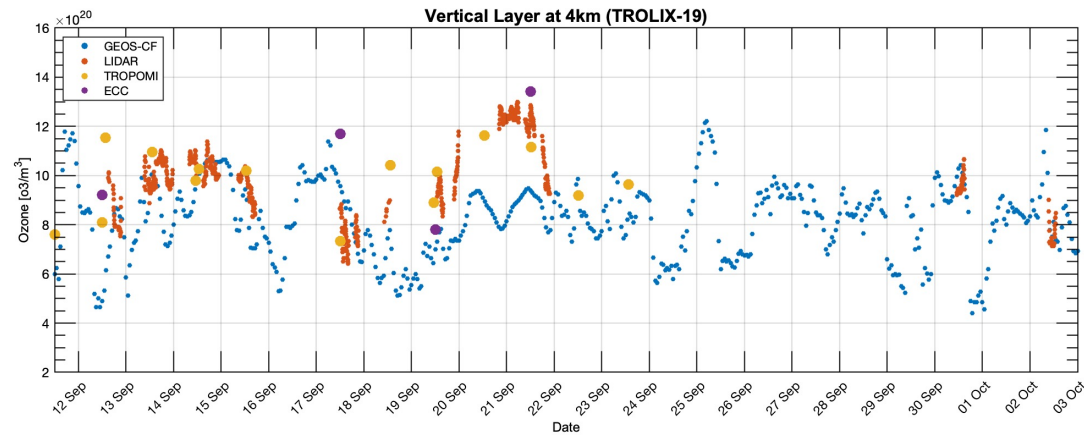


796

797 **Figure 2: Cloud screened TROPOZ lidar retrievals (top panel) and the corresponding GEOS-CF model output (bottom**  
798 **panel) from the closest model grid cell to the CESAR observatory during TROLIX-19 for a) 13 Sep 14-00 UTC, b) 15**  
799 **Sep 09-21 UTC, c) 19 Sep 10-00 UT, d) 20 Sep 16-00 UT, e) 21 Sep 0-3 UT, f) 21 Sep 16-00UT, and g) 02 Oct 04-14 UT.**  
800 **Pink dots are overlaid to indicate the simulated tropopause altitude based on a blended estimate (TROPPB).**

801  
802  
803  
804  
805  
806  
807  
808  
809  
810  
811  
812  
813  
814  
815  
816  
817

818  
819  
820  
821  
822  
823  
824  
825  
826  
827  
828  
829  
830

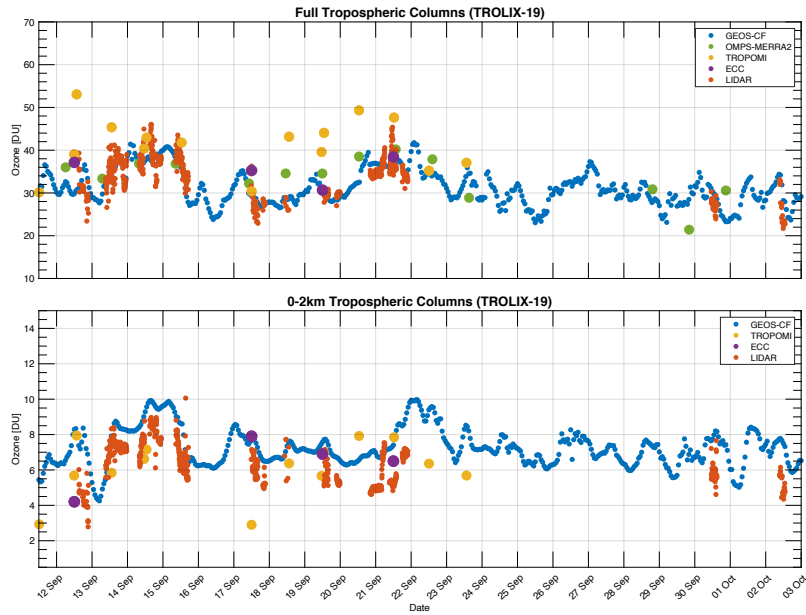


831  
832

833 **Figure 3: Ozone number density values for the TROPOZ lidar, GEOS-CF mode, TROPOMI and electro-chemical cell**  
834 **(ECC) ozonesondes at the 4km layers/levels. The layer was calculated to match the closest representative vertical layer**  
835 **of the GEOS-CF for consistent intercomparison. Data is averaged in a 500m layer from 3.94 km to 4.44 km AGL.**

836  
837  
838  
839  
840  
841  
842  
843

844  
845  
846  
847  
848  
849  
850  
851  
852  
853  
854  
855  
856

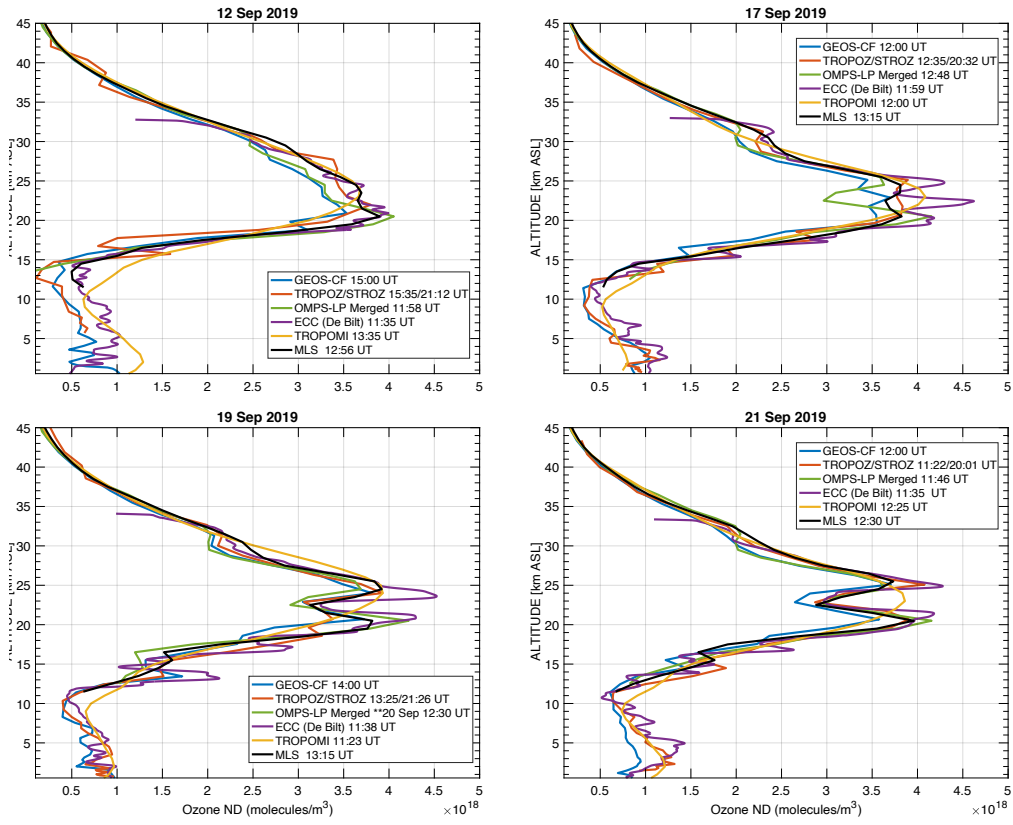


857

858 **Figure 4: Full tropospheric columns (top panel) and 0-2km tropospheric columns (bottom panel) calculated from**  
859 **GEOS-CF, OMPS-MERRA2 (full column only), TROPOMI, Lidar and ECC. Data where reflectivity was greater than**  
860 **0.6 was excluded to remove cloud interference.**

861  
862  
863  
864  
865  
866  
867  
868  
869  
870  
871  
872

873  
874  
875  
876  
877  
878  
879  
880



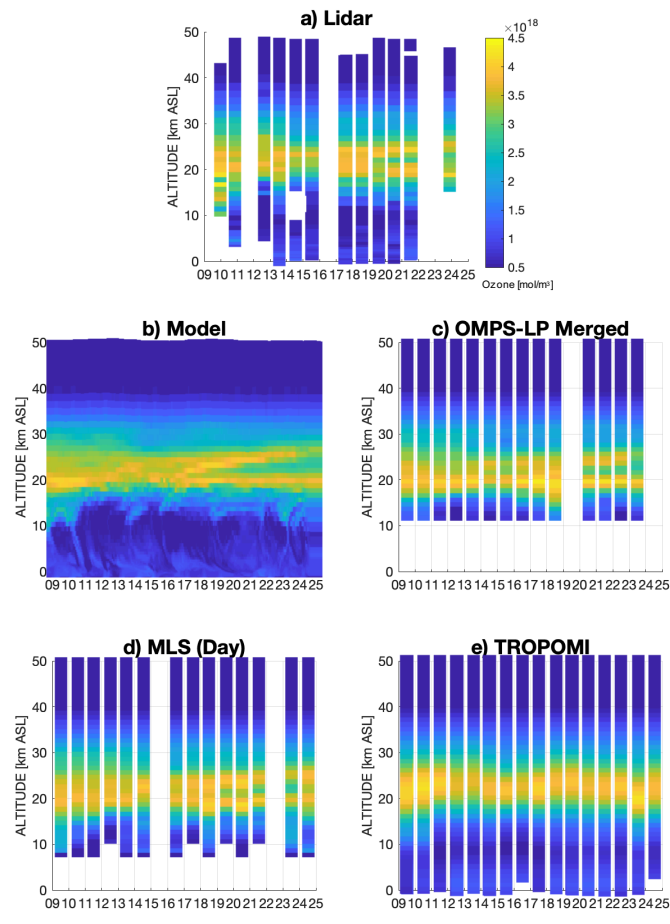
881  
882

883 **Figure 5: GEOS-CF, Lidar, OMPS-LP, ECC, TROPOMI, and MLS ozone profile comparisons for 12 Sep, 17- Sep, 19**  
884 **Sep, and 21 Sep 2019. These days were selected as days within the campaign that had an ECC launch from De Bilt.**

885  
886  
887  
888  
889  
890



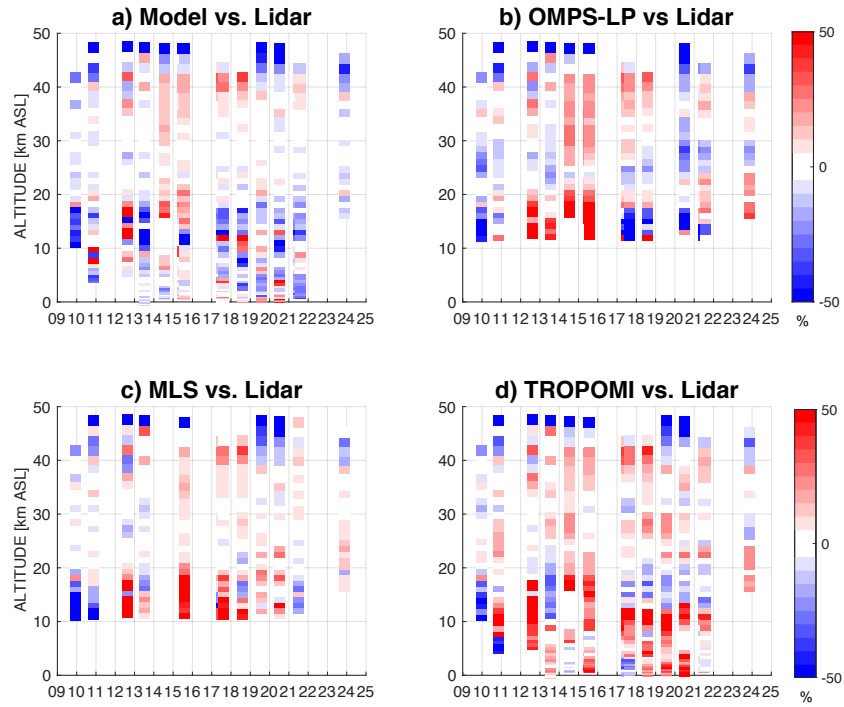
891  
892  
893  
894  
895  
896  
897



898  
899  
900  
901  
902

Figure 6: Ozone number densities across all platforms for the TROLIX-19 time period from the hybrid lidar dataset (Figure 6a), GEOS-CF (Figure 6b), OMPS-LP (Figure 6c), MLS (Figure 6d), TROPOMI (Figure 6e). The x-axis as day of September 2019.

903  
904  
905  
906  
907  
908  
909  
910  
911  
912  
913  
914  
915



916

917 **Figure 7: Differences in ozone number densities across all platforms for the TROLIX-19 time period for Model (Figure**  
918 **7a), OMPS-LP (Figure 7b), MLS (Figure 7c), and TROPOMI (Figure 7d). The x-axis as day of September 2019.**

919

920

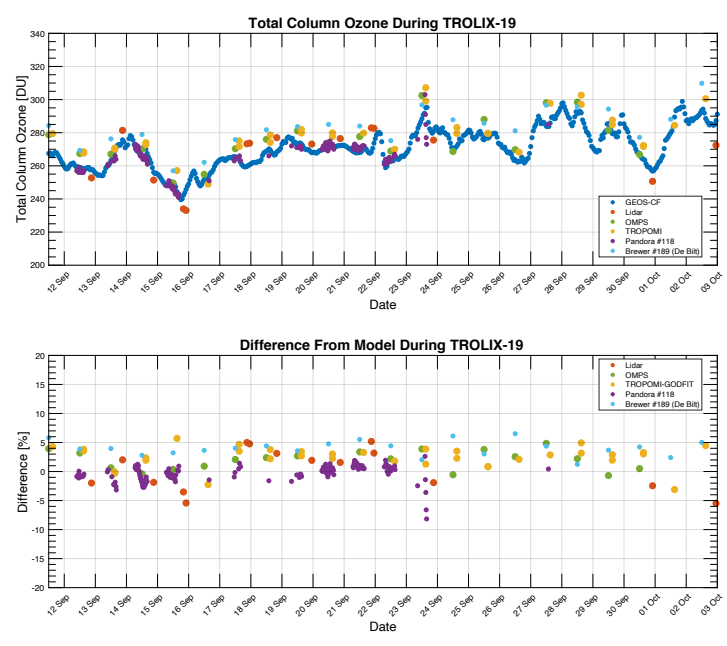
921

922

923

924

925  
926  
  
927  
  
928  
  
929  
  
930  
  
931  
  
932



933  
  
934  
  
935  
  
936

---

Figure 8: Total Ozone columns (top panel) and percent differences (bottom panel) as compared to the model observations for GEOS-CF, lidar, OMPS, TROPOMI, Pandora, and Brewer.